AGU PUBLICATIONS

Geophysical Research Letters

RESEARCH LETTER

10.1002/2016GL068794

Key Points:
- Forest carbon turnover rate is derived from remote sensing-based products of net primary production and biomass
- In boreal forests turnover rate is related to climatic conditions favoring frost stress effects on mortality
- In temperate forests turnover rate is related to climatic conditions favoring drought and insect outbreaks

Supporting Information:
- Supporting Information S1

Correspondence to:
M. Thurner,
martin.thurner@aces.su.se

Citation:
Thurner, M., C. Beer, N. Carvalhais, M. Forkel, M. Santoro, M. Tum, and C. Schmullius (2016), Large-scale variation in boreal and temperate forest carbon turnover rate related to climate, *Geophys. Res. Lett.*, *43*, 4576–4585, doi:10.1002/2016GL068794.

Received 21 MAR 2016
Accepted 20 APR 2016
Accepted article online 25 APR 2016
Published online 14 MAY 2016

Large-scale variation in boreal and temperate forest carbon turnover rate related to climate

Martin Thurner[1,2], Christian Beer[1], Nuno Carvalhais[2,3], Matthias Forkel[2,4], Maurizio Santoro[5], Markus Tum[6], and Christiane Schmullius[7]

[1]Department of Environmental Science and Analytical Chemistry (ACES) and the Bolin Centre for Climate Research, Stockholm University, Stockholm, Sweden, [2]Max Planck Institute for Biogeochemistry, Jena, Germany, [3]CENSE, Departamento de Ciências e Engenharia do Ambiente, Faculdade de Ciências e Tecnologia, Universidade NOVA de Lisboa, Caparica, Portugal, [4]Now at Department of Geodesy and Geoinformation, Research Group Remote Sensing, Technische Universität Wien, Vienna, Austria, [5]Gamma Remote Sensing, Gümligen, Switzerland, [6]German Aerospace Center (DLR), German Remote Sensing Data Center (DFD), Wessling, Germany, [7]Department of Earth Observation, Institute of Geography, Friedrich Schiller University, Jena, Germany

Abstract Vegetation carbon turnover processes in forest ecosystems and their dominant drivers are far from being understood at a broader scale. Many of these turnover processes act on long timescales and include a lateral dimension and thus can hardly be investigated by plot-level studies alone. Making use of remote sensing-based products of net primary production (NPP) and biomass, here we show that spatial gradients of carbon turnover rate (*k*) in Northern Hemisphere boreal and temperate forests are explained by different climate-related processes depending on the ecosystem. *k* is related to frost damage effects and the trade-off between growth and frost adaptation in boreal forests, while drought stress and climate effects on insects and pathogens can explain an elevated *k* in temperate forests. By identifying relevant processes underlying broadscale patterns in *k*, we provide the basis for a detailed exploration of these mechanisms in field studies, and ultimately the improvement of their representations in global vegetation models (GVMs).

1. Introduction

The response of forests to climate change is among the largest uncertainties in the climate-carbon cycle feedback [*Bonan*, 2008]. Especially carbon turnover processes are considered to contribute substantially to the uncertainty of the land carbon balance projected by global vegetation models (GVMs) [*McDowell et al.*, 2011; *Friend et al.*, 2014], whereas shortcomings in the representation of mortality mechanisms in Earth System Models participating in the Coupled Model Intercomparison Project Phase 5 (CMIP5) are likely leading to an underestimation of these effects [*Koven et al.*, 2015]. The concept of *k* represents several ecosystem processes that control the time at which carbon is lost from the system, such as background mortality (including litterfall, root exudates, and herbivory), mortality by disturbances, and forest management. There exists a huge variety of assumptions concerning the processes underlying the large-scale variation in *k*, including different dependencies to climate or competition [*McDowell et al.*, 2011]. At global and regional scales, a positive correlation between forest background mortality and net primary production (NPP) [*Stephenson et al.*, 2011] has been reported. On the other hand, minimum winter temperature is considered the most important bioclimatic limit determining the global distribution of (tree) species [*Sakai and Weiser*, 1973; *Woodward and Williams*, 1987; *Harrison et al.*, 2010]. Different species have different cold tolerances, below which mortality levels increase as a result of complex effects of low temperatures, including biochemical and structural effects of freezing plant and soil water on plant cells, which can be modified by snow cover insulation [*Sakai and Larcher*, 1987].

In contrast, extreme climate events contribute to higher levels of forest mortality by disturbances. Especially drought events have been found to result in significantly higher mortality [*Allen et al.*, 2010], with numerous examples in temperate and boreal forests. For instance, regionally elevated forest mortality in the southwest USA is very likely driven by drought stress, implying both catastrophic mortality events [*Breshears et al.*, 2005] and long-term forest background mortality [*Williams et al.*, 2010]. Increased forest mortality as a consequence of warm and dry conditions has also been observed in western Europe [*Bréda et al.*, 2006]. Furthermore, drought and heat enhance the risk of both insect outbreaks and fire events [*Williams et al.*, 2010]. In North America, insect outbreaks are considered to be the most important disturbance agent [*Logan et al.*, 2003].

Climate change is supposed to influence the frequency and severity of extreme climate events and thus potentially contributes to increased mortality rates [*Reichstein et al*., 2013].

Recently, the dependency of global patterns of whole-ecosystem carbon turnover time, which is strongly driven by soil carbon stocks, on temperature and precipitation has been shown [*Carvalhais et al*., 2014]. Here we focus specifically on vegetation carbon turnover in Northern Hemisphere boreal and temperate forests in order to identify key mechanisms that govern the large-scale variation in k in these ecosystems. Under the assumption of steady state, the influx (NPP) to the forest carbon reservoir (biomass) is balanced with its outflux (biomass $\times k$). Thus, the forest k can be derived from the flux and the reservoir size:

$$k = \frac{\mathrm{NPP}}{\mathrm{Biomass}} \tag{1}$$

k (year^{-1}) denotes the rate at which carbon is released from the forest vegetation pools. It equals the reciprocal of carbon residence time or turnover time, which denotes the average time a carbon atom is stored in forest biomass.

In this study, broadscale forest biomass [*Thurner et al*., 2014; *Santoro et al*., 2011; *Santoro et al*., 2015] and NPP [*Running et al*., 2004; *Zhao et al*., 2005; *Zhao and Running*, 2010] data sets based on remote sensing data are used to calculate the average forest k at 0.5° spatial resolution during 2001–2010, covering boreal and temperate forests of the Northern Hemisphere (30–80°N). Therefore, and in contrast to plot-level field studies, the presented approach allows for a spatially comprehensive analysis over large areas. Furthermore, the data match the required spatial scale at which processes are represented in current GVMs, circumventing uncertainty related to upscaling of field study results.

Following *Carvalhais et al*. [2014], the k derived here is to be understood as an apparent property of the forest ecosystem rather than an inherent vegetation property. Our assumption of steady state involves that the influx (NPP) to vegetation carbon pools in boreal and temperate forests is balanced with their outflux, comprising litterfall as well as disturbances, at a landscape scale over the long term. At these spatial and temporal scales, disturbance regimes and their associated return intervals are integral parts determining steady state conditions in a forest ecosystem. The validity of the steady state assumption cannot be verified using observations of the carbon outflux of forest vegetation pools, since these measurements do not exist at the required spatial and temporal scales. Nevertheless, GVMs can be applied to investigate the difference between turnover rates derived from carbon influx and outflux (see section 4). Such an experiment also helps to understand whether climate change-related alterations in the proportions of carbon influxes and outfluxes could potentially influence our results.

2. Materials and Methods

2.1. Observation-Based Forest Carbon Turnover Rate

Vegetation carbon density (kg C m^{-2}) of northern boreal and temperate forests in 2010 was recently mapped at 0.01° resolution [*Thurner et al*., 2014; *Santoro et al*., 2011; *Santoro et al*., 2015]. This measure is called biomass in this study. Based on radar remote sensing (hypertemporal Envisat/Advanced Synthetic Aperture Radar (ASAR) C band data) derived growing stock volume information [*Santoro et al*., 2011, 2015], biomass was derived making use of databases on wood density and allometric relationships. Intercomparison of this product and inventory-based biomass data sets showed strong agreement at regional scales across Russia, the USA, and Europe [*Thurner et al*., 2014], demonstrating the validity of this product at such spatial resolution. This biomass estimate accounts for stem, branch, root, and foliage biomass.

The Moderate-resolution Imaging Spectroradiometer (MODIS) MOD17 product provides information on NPP with a spatial resolution of 1 km [*Running et al*., 2004; *Zhao et al*., 2005; *Zhao and Running*, 2010] (obtained from http://www.ntsg.umt.edu/project/mod17) and was reprojected to geographic coordinates at 0.01° resolution. Average long-term NPP was derived for the period 2001–2010 in order to decrease the influence of interannual variability. This NPP product is based on several satellite-derived (MODIS fraction of photosynthetically active radiation absorbed by the vegetation (fPAR), land cover, and leaf area index (LAI)) and meteorological input data sets and accounts for gross primary production (GPP), maintenance, and growth respiration of woody components and living tissue (for details, see *Heinsch et al*. [2003]). Moreover, we applied an alternative NPP product (BETHY/DLR NPP [*Wißkirchen et al*., 2013; *Tum et al*., 2016])

and an additional proxy of NPP derived from a data-driven estimate of GPP [*Beer et al*., 2010] in order to assess the influence of the uncertainty in NPP on our results (see section 4; Texts S2 and S3 and corresponding Figures S3–S14 in the supporting information).

Both biomass and NPP data sets were aggregated to 0.5° resolution prior to calculating k, taking into account only forested pixels according to the GLC2000 land use/land cover map [*Joint Research Centre* (*JRC*), 2003]. Additionally, the MODIS MOD12 land cover classification [*Friedl et al*., 2010] was used for division between forest and nonforest in order to consider only grid cells where the MODIS NPP product has been derived from parameters calibrated to forest biomes [*Heinsch et al*., 2003]. Nonforest pixels were masked out already before aggregation, and only 0.5° grid cells containing at least 40% forest covered grid cells at 0.01° (according to GLC2000) were considered to be dominated by forest and included in the analysis. Aggregation to 0.5° was performed in order to reduce the influence of uncertainties of the biomass, NPP, and land cover products at their original spatial scale.

2.2. Controls of Forest Carbon Turnover Rate

Climate variables presented here include the number of icing days, number of frost days and maximum length of warm-dry periods, but the analysis was not limited to them. Icing days are defined as the annual count of days with a daily maximum (surface air) temperature below 0°C, whereas frost days are the annual count of days with a daily minimum temperature below 0°C. We refer to warm-dry periods as both warm ($T_{max} \geq 10$°C) and dry (without precipitation) consecutive days, and derived their maximum length for each year. Long-term average values (1981–2010) were calculated for all of these variables based on originally daily climate data from the Water and Global Change programme (WATCH) [*Weedon et al*., 2011], which are available at 0.5° resolution. Different leaf types (broadleaf/needleleaf, deciduous/evergreen) and biomes (boreal/temperate) were separated using the land cover map GLC2000 [*JRC*, 2003] and a biome map [*Olson et al*., 2001], respectively.

2.3. Relationships Between Turnover Rate and Climate

The relationships between the observation-based k and the climatic variables were investigated at 0.5° resolution. In general, we found exponential functions of the form

$$k = k_{base} + e^{\frac{x - C_{lim}}{m}} \tag{2}$$

best suited (in terms of Modelling Efficiency (MEF) [*Nash and Sutcliffe*, 1970] and ecological interpretability) to model these relationships. MEF is calculated as the variance of the residuals (difference of observed (obs) and modeled (sim) k) over the variance in the observed values:

$$\mathrm{MEF} = 1 - \frac{\Sigma(\mathrm{obs} - \mathrm{sim})^2}{\Sigma(\mathrm{obs} - \mathrm{mean}(\mathrm{obs}))^2} \tag{3}$$

While a negative MEF indicates that the mean of the observations is a better predictor than the model, a MEF of 1 corresponds to a perfect match between model and observations [*Nash and Sutcliffe*, 1970].

k is modeled as a function of a climate variable x, estimating the parameters describing the base turnover rate k_{base}, which is the turnover rate occurring without influence of the climate variable, the climatic limit C_{lim} where the turnover rate becomes $k_{base} + 1$, and a parameter m defining the slope of the exponential function. These functions were fitted by nonlinear least squares regression in *R* using the port algorithm [*Bates and Watts*, 1988], which allows defining parameter lower and/or upper boundaries beforehand.

3. Results

Large-scale forest k shows clear spatial gradients especially toward the northern edges of boreal and toward the southern edges of temperate forests (Figure 1). In those regions, the estimated k can increase to values above 0.2 year^{-1} but is mostly below 0.15 year^{-1}, with a mean turnover rate of 0.092 year^{-1} in Northern Hemisphere boreal and temperate forests (cf. Text S1 in the supporting information). NPP in general increases with annual temperature and precipitation; although in ecosystems limited by either temperature or precipitation, this relationship has not been observed using a comprehensive database of direct NPP measurements [*Luyssaert et al*., 2007]. While NPP in boreal regions is mostly limited by temperature, in temperate forests radiation and temperature in winter, temperature in spring and precipitation in summer can be the climatic

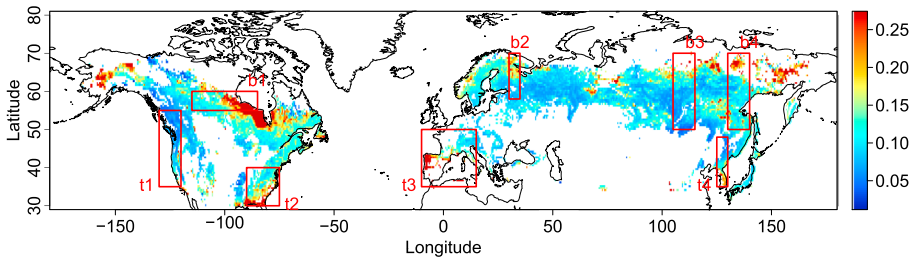

Figure 1. Spatial patterns of forest k (year^{-1}) as the ratio of MODIS NPP [*Running et al.*, 2004; *Zhao et al.*, 2005; *Zhao and Running*, 2010] over biomass [*Thurner et al.*, 2014; *Santoro et al.*, 2011; *Santoro et al.*, 2015], for all areas with at least 40% forest cover (according to GLC2000 land cover data set [*JRC*, 2003]; additional use of MODIS MOD12 land cover classification [*Friedl et al.*, 2010]). Red boxes show selected transects (Table S1 in the supporting information): b1, Canada; b2, Karelia/western Russia; b3, central Siberia/Baikal; b4, eastern Siberia; t1, western North America; t2, southeastern North America; t3, southwestern Europe; t4, northeastern China/Korea.

factors determining the upper bound of NPP [*Running et al.*, 2004]. Similar temperature and precipitation-driven gradients in NPP are reproduced by GVMs [*Cramer et al.*, 1999]. However, in this study we find increases in k with frost (boreal forests) and drought (temperate forests), respectively. Hence, these gradients cannot be driven by gradients in NPP; they rather must be related to other processes which directly cause gradients in biomass, i.e., carbon turnover processes.

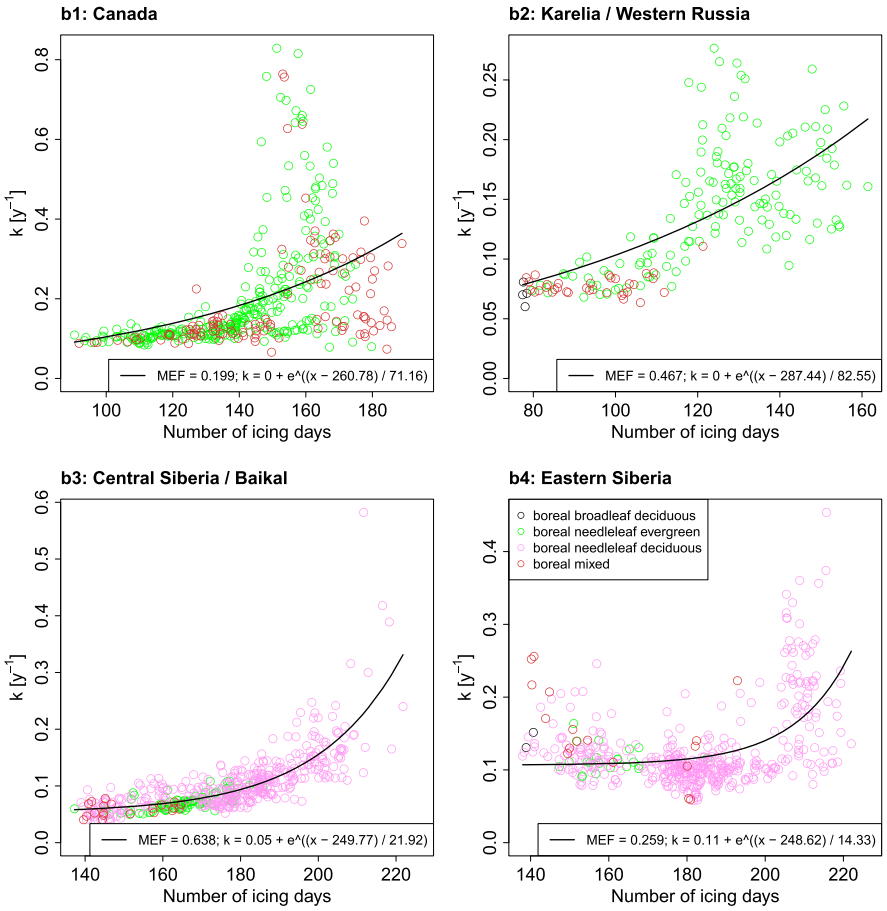

Figure 2. k as a function of the number of icing days during a year in boreal forest transects. Points correspond to all 0.5° grid cells within the specified transects (cf. Table S1 in the supporting information) with at least 40% forest cover (according to GLC2000 land cover data set [*JRC*, 2003]; additional use of MODIS MOD12 land cover classification [*Friedl et al.*, 2010]).

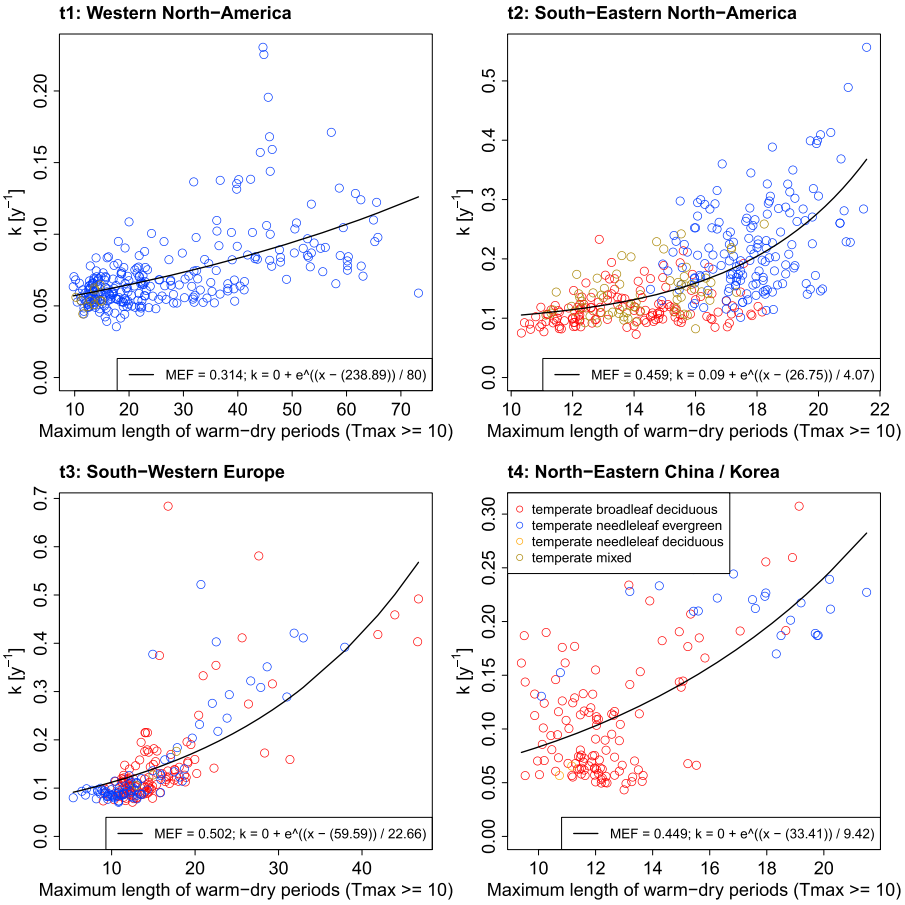

Figure 3. *k* as a function of the maximum length of warm-dry periods (in days) during a year in temperate forest transects. Points correspond to all 0.5° grid cells within the specified transects (cf. Table S1 in the supporting information) with at least 40% forest cover (according to GLC2000 land cover data set [*JRC*, 2003]; additional use of MODIS MOD12 land cover classification [*Friedl et al*., 2010]).

k increases with the number of icing days in boreal forests (Figure 2; for transect definition, see Table S1 in the supporting information). Also, other climate variables related to winter temperatures and length (e.g., minimum temperature of the coldest month and growing season length) show similar patterns (see Tables S2 and S3 in the supporting information) due to their high correlation. Although boreal needleleaf trees are supposed to be able to survive winter temperatures up to −60°C to −70°C, extremely cold resistant tree species require a long dormancy during winter and bud burst is occurring very late in spring. Hence, extremely cold and long winters lead to a reduced growing season length [*Harrison et al*., 2010]. Short growing seasons in turn prevent trees from developing the required resistance to frost and winter desiccation [*Tranquillini*, 1979]. Frost-induced mortality mechanisms include xylem embolism [*Sperry and Sullivan*, 1992], desiccation due to strong winds or frozen soil [*Sakai and Larcher*, 1987], physical damage caused by ice storms [*Sun et al*., 2012], and increased vulnerability to wind throws due to decreased forest vitality [*Schlyter et al*., 2006].

In temperate forests, *k* increases with the length of both warm and dry consecutive days (Figure 3). In western North America (t1) and southwestern Europe (t3), there is also a strong increase in *k* for extremely low precipitation levels during the warmest quarter of the year (cf. Table S2 in the supporting information). However, in southeastern North America (t2) and northeastern China/Korea (t4) this relationship cannot be observed, due to relatively high precipitation amounts during summer periods in those regions. The observed relationship can probably be explained by drought stress, which has been reported to lead to an increased mortality in forests all over the world [*Allen et al*., 2010]. Mechanisms of tree death caused by drought stress are still under debate, including theories of carbon starvation and hydraulic failure [*McDowell et al*., 2011]. Furthermore, high

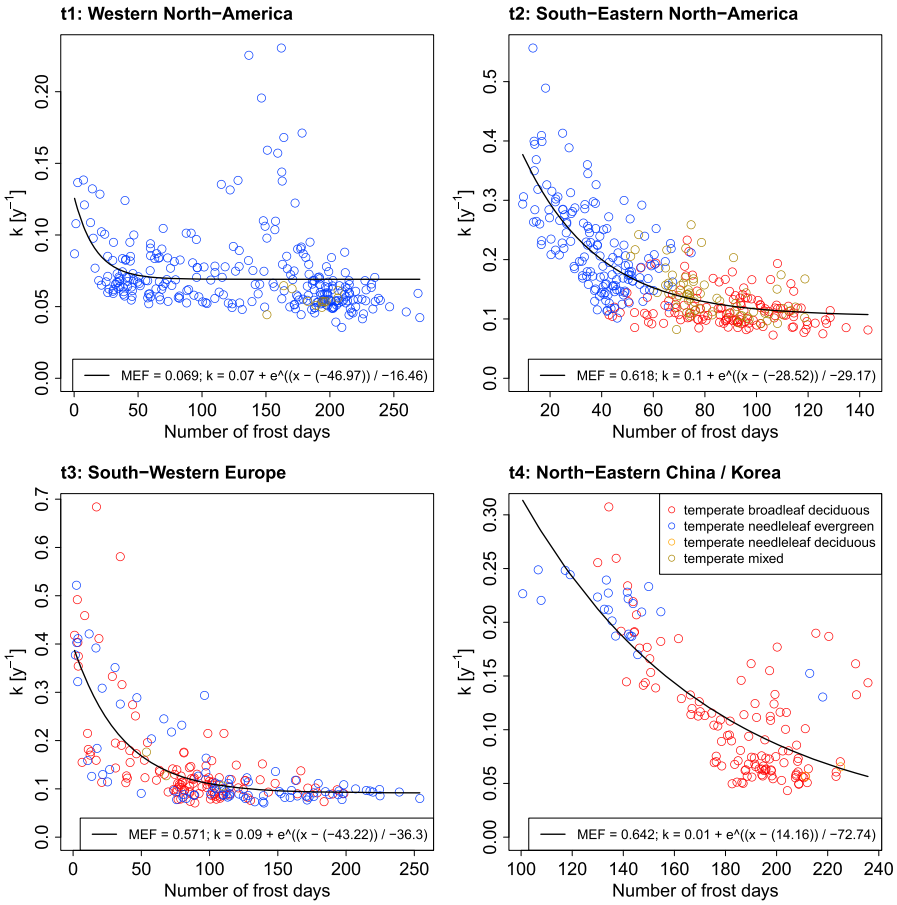

Figure 4. *k* as a function of the number of frost days during a year in temperate forest transects. Points correspond to all 0.5° grid cells within the specified transects (cf. Table S1 in the supporting information) with at least 40% forest cover (according to GLC2000 land cover data set [*JRC*, 2003]; additional use of MODIS MOD12 land cover classification [*Friedl et al.*, 2010]).

temperatures together with low precipitation increase the fire risk and have the potential to weaken trees and make them more susceptible to insect attacks [*Williams et al.*, 2010; *Reichstein et al.*, 2013; *Raffa et al.*, 2008]. In contrast to temperate forests, we did not identify a consistent relationship between drought and *k* in boreal forests.

Moreover, a higher *k* is observed in temperate forests for areas with a lower number of frost days per year (Figure 4). These findings may be related to the importance of winter temperature for the survival of insects and pathogens. Minimum winter temperature is known to be the most important control of insect survival during winter [*Bale et al.*, 2002], bark beetles being studied most intensively [*Safranyik and Carroll*, 2006]. In case minimum winter temperatures do not fall below critical lower limits, some insects, for instance, bark beetles, can proceed in their generation cycle [*Williams and Liebhold*, 2002]. In general, increased temperatures can allow them to produce several generations during 1 year, favoring an epidemic outbreak if also other conditions are met [*Raffa et al.*, 2008]. Similar controls have been observed for pathogens native to temperate forests [*Bergot et al.*, 2004; *Chavarriaga et al.*, 2007], although research on the importance of pathogens is underrepresented. In addition to increases in *k* and consequent reductions in forest biomass, bark beetle attacks have been found to lead to increases in NPP at landscape level over the long term, since the beetles prefer attacking the largest trees, enabling surviving understory and smaller trees to grow faster due to reduced competition for light, water, and nutrients [*Raffa et al.*, 2008]. While increases in mortality might be best explained by drought stress in water-limited temperate forests, mortality in energy-limited temperate forests might be mostly related to insects and pathogens [*Das et al.*, 2013]. Multivariate exponential models adding the influence of both predictor variables lead to a significant increase in MEF in region t3 and a slight increase in the other transects (see Table S4 in the supporting information).

Parameters of the relationships of k to climate variables, i.e., the climatic limit and steepness of the increase in k, are considerably different between regions. On the other hand, only small differences in the low levels of k are observed over a wide climatic range within some regions, until a climatic limit is reached, where k increases strongly with increasingly extreme climate. For example, in central Siberia/Baikal (b3) and eastern Siberia (b4), k appears to considerably rise only for more extreme winter lengths and temperatures, but then with a steeper gradient compared to Canada (b1) and Karelia/western Russia (b2, Figure 2). We suppose that in addition to possible interactions of the effects of the investigated climate variables and other environmental conditions on k, differences in adaptation strategies are responsible for these patterns. For instance, geographically marginal populations, which are used to more extreme climatic conditions, have been found to be more strongly adapted to frost [*Kreyling et al*., 2014] and drought [*Thiel et al*., 2014] than central populations. The response of mortality rates to drought differs between species and may also change over time, potentially leading to changes in species composition over the long term, benefiting the better adapted or adapting species [*Barbeta et al*., 2013]. Adaptation itself is driven by a trade-off between growth and mortality by either frost in boreal [*Schreiber et al*., 2013] or drought in temperate forests [*Thiel et al*., 2014]. Our results support evidence that the spatial distribution of leaf types can be considered a direct consequence of adaptation to climate [*Sakai and Weiser*, 1973; *Woodward and Williams*, 1987; *Harrison et al*., 2010], since we did not find substantially different deviations from the relationships between k and climate depending on the leaf type (Figures 2–4).

4. Discussion

The presented long-term k accounts for both turnover of woody forest components and turnover of living tissue, including foliage and fine roots. In the absence of other studies integrating over both woody and living tissue aboveground and belowground, we compared our variance in k ((area-weighted) median = 0.095 year^{-1}, first quartile = 0.076 year^{-1}, third quartile = 0.120 year^{-1}) to the variance in turnover rates derived from the Luyssaert database [*Luyssaert et al*., 2007] (median = 0.053 year^{-1}, first quartile = 0.034 year^{-1}, third quartile = 0.090 year^{-1}), integrating over boreal and temperate forests in the whole study area (Figure S1 in the supporting information). Although this evaluation seems to indicate an overestimation of k in our study, a comparison to the variance in turnover rate derived from the Luyssaert database has its own shortcomings. Most importantly, in contrast to our estimates of k, the Luyssaert database and also other collections of field measurements do not capture the variety of turnover processes (litterfall and all kinds of disturbances) at landscape scale over long time periods. Field measurements are unlikely to be representative for a 0.5° grid cell and can potentially be biased if they are implemented in largely undisturbed forests. In addition, the Luyssaert database is biased in the spatial distribution of measurement sites. Not many measurements are taken in areas where we observe the highest k, potentially leading to an underestimation of the median k (Figure S2 in the supporting information). Thus, in addition to biases in the applied NPP and biomass data sets, the possible overestimation of our estimated k could likely be explained also by other reasons related to the reference data set. Overall, we found no sufficient data for an independent field-based evaluation of the estimated large-scale spatial patterns of k. Applying a different NPP product (BETHY/DLR NPP [*Wißkirchen et al*., 2013; *Tum et al*., 2016]) does not reveal lower k closer to ranges in field measurements ((area-weighted) median = 0.101 year^{-1}, first quartile = 0.084 year^{-1}, third quartile = 0.122 year^{-1}). Making use of alternative NPP products and an additional proxy of NPP derived from a data-driven estimate of GPP [*Beer et al*., 2010] minimizes effects of the NPP uncertainty and confirms the observed spatial patterns in forest k and their relationship to the presented climatic indices (Text S2 and corresponding Figures S3–S10 in the supporting information). Based on the BETHY/DLR NPP product in addition to MODIS, and the uncertainty in biomass estimated by *Thurner et al*. [2014], we derive a first uncertainty estimate for k (Text S3 and corresponding Figures S11–S14 in the supporting information). Furthermore, an evaluation against upscaled forest inventory NPP estimates at the scale of the administrative units in Russia [*Shvidenko et al*., 2007] indicates that the gradients observed in k cannot be caused by a gradually increasing overestimation of NPP with decreasing NPP (Figure S15 in the supporting information). Although both MODIS and BETHY/DLR NPP products include models of GPP and plant respiration, their main drivers are biophysical variables obtained from remote sensing, particularly fPAR and LAI.

Potentially other processes than suggested may cause indirectly the observed relationships of *k* to climatic indices. These processes can contribute to the noise in the climate-*k* relationships; however, most of such potential confounding factors can hardly explain the spatial gradients. For instance, there is no evidence that forest management is more extensive toward the northern boundary of boreal forests or toward drier regions of temperate forests. Also, forest fires are considered to be related to drought conditions (and included in our hypothesis 2 below), but due to stochastic influences on the spatial occurrence and spread of fires, we do not find that burned area or the time since last fire are responsible for observed broadscale gradients in *k* (Figures S16 and S17 in the supporting information). In addition, we did not detect consistent relationships of *k* to different investigated soil-related variables in our study regions, with the exception of a weak positive correlation between *k* and the topsoil organic carbon content in boreal forest transects (Table S5 in the supporting information).

Furthermore, differences in the deviation from steady state between grid cells can potentially have an influence on our results, but again, this would require a spatial correlation between forest successional state and the investigated climate variables. For instance, it is possible that changes in winter length and temperature in the northern edge of boreal forests lead to a shift of the treeline farther to the north, and thus, forests are in a successional state [*Urban et al*., 2014], resulting in a currently higher *k* compared to steady state forests. However, at the spatial scale of our study, *k* spatial patterns simulated by a set of GVMs do not substantially differ when we calculate *k* based on outflux (carbon turnover from vegetation to soil and atmosphere) instead of influx (NPP; Table S6 in the supporting information).

The variance in *k* in the investigated boreal forest transects is mostly originating from a higher variance in biomass, while the variance in NPP is comparatively lower. On the other hand, we did not find a consistent difference between the variance in NPP and the variance in biomass in the selected temperate forest transects (Table S7 in the supporting information). In boreal forests, spatial gradients in tree cover correlate with gradients in climate and can potentially introduce a bias in MODIS NPP (Figures S18–S21 in the supporting information). In order to not include grid cells with only sparse forest cover in this analysis, we applied different land cover products and an additional forest cover threshold. On the other hand, tree cover in mainly unmanaged boreal forest regions can also be interpreted as a consequence of climatic conditions and a result of climate-induced *k*.

Not accounting for climate dependencies of biomass allocation [*Reich et al*., 2014] may possibly affect the presented gradients, since different biomass compartments imply unequal *k*. However, the proportions of foliage and root carbon, the two compartments with significantly higher *k* compared to stem and branches carbon, are reported to be related to mean annual temperature in opposite directions [*Reich et al*., 2014]. In addition, using an exhaustive database based on field measurements, we do not find strong correlations between biomass allometry and the investigated climate variables (Figures S22 and S23 in the supporting information). Hence, we conclude that our observed *k*-climate relationships are unlikely mainly attributable to climate dependencies of allocation; nevertheless, spatial patterns in allocation may influence our results, for instance, if driven by spatial gradients in light or nutrient availability [*Poorter et al*., 2012].

Based on novel remote sensing products used in this study, we presented evidence for the following hypotheses:

1. The spatial variation of *k* in boreal forests is related to frost damage effects and the trade-off between growth and frost adaptation.
2. The spatial variation of *k* in temperate forests can be explained by climatic conditions favoring drought and insect outbreaks.
3. Differences in adaptation to frost or drought and/or interactions with other environmental conditions modify these relationships in different ecoregions.

For the first time, we were able to study the effects of interacting mortality processes and their relevance at continental scale. Future studies will benefit from multitemporal observations of forest biomass, making estimates of *k* independent of the steady state assumption. Our findings are important for identifying processes which need to be considered by GVMs and can also be used for their evaluation. This will lead to improvements of predicted carbon stock spatial patterns and future carbon cycle dynamics in response to climate change [*Delbart et al*., 2010; *Galbraith et al*., 2013]. However, the differences in the observed *k*-climate relationships between regions, which might be explained by adaptation or interactions with other environmental variables, require a detailed exploration of the underlying mechanisms in field studies, before they can be reproduced by GVMs.

Acknowledgments

The MODIS NPP product (MOD17) provided by the Numerical Terradynamic Simulation Group of the University of Montana contributed significantly to this work. Data obtained from the CD-ROM/Web site titled Russian Forests and Forestry provided by the International Institute for Applied Systems Analysis (IIASA) have been used for an evaluation of applied NPP products. For his help in data processing we want to acknowledge Ulrich Weber (Max Planck Institute for Biogeochemistry Jena). We are very grateful to Martin Jung, Franziska Schrodt (both Max Planck Institute for Biogeochemistry Jena), and Christian Reick (Max Planck Institute for Meteorology Hamburg) for their ideas contributing to this work. Nuno Carvalhais acknowledges funding from NOVA grant UID/AMB/04085/2013.

References

Allen, C. D., et al. (2010), A global overview of drought and heat-induced tree mortality reveals emerging climate change risks for forests, *For. Ecol. Manage.*, *259*(4), 660–684.

Bale, J. S., et al. (2002), Herbivory in global climate change research: Direct effects of rising temperature on insect herbivores, *Glob. Chang. Biol.*, *8*, 1–16.

Barbeta, A., R. Ogaya, and J. Penuelas (2013), Dampening effects of long-term experimental drought on growth and mortality rates of a Holm oak forest, *Glob. Chang. Biol.*, *19*, 3133–3144.

Bates, D. M., and D. G. Watts (1988), *Nonlinear Regression Analysis and Its Applications*, Wiley, New York.

Beer, C., et al. (2010), Terrestrial gross carbon dioxide uptake: Global distribution and covariation with climate, *Science*, *329*(5993), 834–838.

Bergot, M., E. Cloppet, V. Perarnaud, M. Deque, B. Marcais, and M.-L. Desprez-Loustau (2004), Simulation of potential range expansion of oak disease caused by Phytophthora cinnamomi under climate change, *Glob. Chang. Biol.*, *10*(9), 1539–1552.

Bonan, G. B. (2008), Forests and climate change: Forcings, feedbacks, and the climate benefits of forests, *Science*, *320*(5882), 1444–1449.

Bréda, N., R. Huc, A. Granier, and E. Dreyer (2006), Temperate forest trees and stands under severe drought: A review of ecophysiological responses, adaptation processes and long-term consequences, *Ann. For. Sci.*, *63*(6), 625–644.

Breshears, D. D., et al. (2005), Regional vegetation die-off in response to global-change-type drought, *Proc. Natl. Acad. Sci. U.S.A.*, *102*(42), 15,144–15,148.

Carvalhais, N., et al. (2014), Global covariation of carbon turnover times with climate in terrestrial ecosystems, *Nature*, *514*(7521), 213–217.

Chavarriaga, D., W. J. Bodles, C. Leifert, L. Belbahri, and S. Woodward (2007), Phytophthora cinnamomi and other fine root pathogens in north temperate pine forests, *FEMS Microbiol. Lett.*, *276*(1), 67–74.

Cramer, W., D. W. Kicklighter, A. Bondeau, B. Moore III, G. Churkina, B. Nemry, A. Ruimy, A. L. Schloss, and The Participants of the Potsdam NPP Model Intercomparison (1999), Comparing global models of terrestrial net primary productivity (NPP): Overview and key results, *Glob. Chang. Biol.*, *5*(Suppl. 1), 1–15.

Das, A. J., N. L. Stephenson, A. Flint, T. Das, and P. J. van Mantgem (2013), Climatic correlates of tree mortality in water- and energy-limited forests, *PLoS One*, *8*(7), 1–11.

Delbart, N., P. Ciais, J. Chave, N. Viovy, Y. Malhi, and T. Le Toan (2010), Mortality as a key driver of the spatial distribution of aboveground biomass in Amazonian forest: Results from a dynamic vegetation model, *Biogeosciences*, *7*(10), 3027–3039.

Friedl, M. A., D. Sulla-Menashe, B. Tan, A. Schneider, N. Ramankutty, A. Sibley, and X. Huang (2010), MODIS Collection 5 global land cover: Algorithm refinements and characterization of new datasets, *Remote Sens. Environ.*, *114*(1), 168–182.

Friend, A. D., et al. (2014), Carbon residence time dominates uncertainty in terrestrial vegetation responses to future climate and atmospheric CO_2, *Proc. Natl. Acad. Sci. U.S.A.*, *111*(9), 3280–3285.

Galbraith, D., et al. (2013), Residence times of woody biomass in tropical forests, *Plant Ecolog. Divers.*, *6*(1), 139–157.

Harrison, S. P., I. C. Prentice, D. Barboni, K. E. Kohfeld, J. Ni, and J.-P. Sutra (2010), Ecophysiological and bioclimatic foundations for a global plant functional classification, *J. Veg. Sci.*, *21*(2), 300–317.

Heinsch, F. A. et al. (2003), User's guide: GPP and NPP (MOD17A2/A3) products. *NASA MODIS land algorithm*, Version 2.0, December 2.

Joint Research Centre (JRC) (2003), Global Land Cover 2000 database, European Commission, Joint Research Centre. [Available at http://forobs.jrc.ec.europa.eu/products/glc2000/glc2000.php.]

Koven, C. D., J. Q. Chambers, K. Georgiou, R. Knox, R. I. Negron-Juarez, W. J. Riley, V. Arora, V. Brovkin, P. Friedlingstein, and C. D. Jones (2015), Controls on terrestrial carbon feedbacks by productivity versus turnover in the CMIP5 Earth System Models, *Biogeosciences*, *12*, 5211–5228.

Kreyling, J., et al. (2014), Local adaptations to frost in marginal and central populations of the dominant forest tree *Fagus sylvatica L.* as affected by temperature and extreme drought in common garden experiments, *Ecol. Evol.*, *4*(5), 594–605.

Logan, J. A., J. Régnière, and J. A. Powell (2003), Assessing the impacts of global warming on forest pest dynamics, *Front. Ecol. Environ.*, *1*(3), 130–137.

Luyssaert, S., et al. (2007), CO_2 balance of boreal, temperate, and tropical forests derived from a global database, *Glob. Chang. Biol.*, *13*(12), 2509–2537.

McDowell, N. G., D. J. Beerling, D. D. Breshears, R. A. Fisher, K. F. Raffa, and M. Stitt (2011), The interdependence of mechanisms underlying climate-driven vegetation mortality, *Trends Ecol. Evol.*, *26*(10), 523–532.

Nash, J. E., and J. V. Sutcliffe (1970), River flow forecasting through conceptual models: Part I. A discussion of principles, *J. Hydrol.*, *10*, 282–290.

Olson, D. M., et al. (2001), Terrestrial ecoregions of the world: A new map of life on Earth, *BioScience*, *51*(11), 933–938.

Poorter, H., K. J. Niklas, P. B. Reich, J. Oleksyn, P. Poot, and L. Mommer (2012), Biomass allocation to leaves, stems and roots: Meta-analyses of interspecific variation and environmental control, *New Phytol.*, *193*, 30–50.

Raffa, K. F., B. H. Aukema, B. J. Bentz, A. L. Carroll, J. A. Hicke, M. G. Turner, and W. H. Romme (2008), Cross-scale drivers of natural disturbances prone to anthropogenic amplification: The dynamics of bark beetle eruptions, *BioScience*, *58*(6), 501.

Reich, P. B., Y. Luo, J. B. Bradford, H. Poorter, C. H. Perry, and J. Oleksyn (2014), Temperature drives global patterns in forest biomass distribution in leaves, stems, and roots, *Proc. Natl. Acad. Sci. U.S.A.*, *111*(38), 13,721–13,726.

Reichstein, M., et al. (2013), Climate extremes and the carbon cycle, *Nature*, *500*(7462), 287–295.

Running, S. W., R. R. Nemani, F. A. Heinsch, M. Zhao, M. Reeves, and H. Hashimoto (2004), A continuous satellite-derived measure of global terrestrial primary production, *BioScience*, *54*(6), 547–560.

Safranyik, L., and A. L. Carroll (2006), The biology and epidemiology of the mountain pine beetle in lodgepole pine forests, in *The Mountain Pine Beetle: A Synthesis of Biology, Management, and Impacts on Lodgepole Pine*, edited by L. Safranyik and B. Wilson, pp. 3–66 , Natural Resources Canada, Canadian Forest Service, Pacific Forestry Centre, Victoria, BC.

Sakai, A., and C. J. Weiser (1973), Freezing resistance of trees in North America with reference to tree regions, *Ecology*, *54*(1), 118–126.

Sakai, A., and W. Larcher (Eds) (1987), *Frost Survival of Plants: Responses and Adaptation to Freezing Stress*, pp. 321, Springer, Berlin.

Santoro, M., C. Beer, O. Cartus, C. Schmullius, A. Shvidenko, I. McCallum, U. Wegmüller, and A. Wiesmann (2011), Retrieval of growing stock volume in boreal forest using hyper-temporal series of Envisat ASAR ScanSAR backscatter measurements, *Remote Sens. Environ.*, *115*(2), 490–507.

Santoro, M., et al. (2015), Forest growing stock volume of the northern hemisphere: Spatially explicit estimates for 2010 derived from Envisat ASAR, *Remote Sens. Environ.*, *168*, 316–334.

Schlyter, P., I. Stjernquist, L. Bärring, A. M. Jönsson, and C. Nilsson (2006), Assessment of the impacts of climate change and weather extremes on boreal forests in northern Europe, focusing on Norway spruce, *Climate Res.*, *31*, 75–84.

Schreiber, S. G., C. Ding, A. Hamann, U. G. Hacke, B. R. Thomas, J. S. Brouard, and S. Saura (2013), Frost hardiness vs. growth performance in trembling aspen: An experimental test of assisted migration, *J. Appl. Ecol.*, *50*(4), 939–949.

Shvidenko, A., D. Schepaschenko, S. Nilsson, and Y. Bouloui (2007), Semi-empirical models for assessing biological productivity of Northern Eurasian forests, *Ecol. Modell.*, *204*(1-2), 163–179.

Sperry, J. S., and J. E. M. Sullivan (1992), Xylem embolism in response to freeze-thaw cycles and water stress in ring-porous, diffuse porous, and conifer species, *Plant Physiol.*, *100*, 605–613.

Stephenson, N. L., P. J. Van Mantgem, A. G. Bunn, H. Bruner, M. E. Harmon, K. B. O'Connell, D. L. Urban, and J. F. Franklin (2011), Causes and implications of the correlation between forest productivity and tree mortality rates, *Ecol. Monogr.*, *81*(4), 527–555.

Sun, Y., L. Gu, R. E. Dickinson, and B. Zhou (2012), Forest greenness after the massive 2008 Chinese ice storm: Integrated effects of natural processes and human intervention, *Environ. Res. Lett.*, *7*(3), 035702.

Thiel, D., J. Kreyling, S. Backhaus, C. Beierkuhnlein, C. Buhk, K. Egen, G. Huber, M. Konnert, L. Nagy, and A. Jentsch (2014), Different reactions of central and marginal provenances of Fagus sylvatica to experimental drought, *Eur. J. For. Res.*, *133*(2), 247–260.

Thurner, M., et al. (2014), Carbon stock and density of northern boreal and temperate forests, *Glob.Ecol. Biogeogr.*, *23*(3), 297–310.

Tranquillini, W. (1979), *Physiological Ecology of the Alpine Timberline: Tree Existence at High Altitudes With Special Reference to the European Alps*, Springer, Berlin.

Tum, M., J. N. Zeidler, K. P. Günther, and T. Esch (2016), Global NPP and straw bioenergy trends for 2000-2014, *Biomass Bioenergy*, *90*, 230–236.

Urban, M., M. Forkel, J. Eberle, C. Hüttich, C. Schmullius, and M. Herold (2014), Pan-Arctic climate and land cover trends derived from multi-variate and multi-scale analyses (1981–2012), *Remote Sens.*, *6*(3), 2296–2316.

Weedon, G. P., S. Gomes, P. Viterbo, W. J. Shuttleworth, E. Blyth, H. Österle, J. C. Adam, N. Bellouin, O. Boucher, and M. Best (2011), Creation of the WATCH forcing data and its use to assess global and regional reference crop evaporation over land during the twentieth century, *J. Hydrometeorol.*, *12*(5), 823–848.

Williams, A. P., C. D. Allen, C. I. Millar, T. W. Swetnam, J. Michaelsen, C. J. Still, and S. W. Leavitt (2010), Forest responses to increasing aridity and warmth in the southwestern United States, *Proc. Natl. Acad. Sci. U.S.A.*, *107*(50), 21,289–21,294.

Williams, D. W., and A. M. Liebhold (2002), Climate change and the outbreak ranges of two North American bark beetles, *Agric. For. Entomol.*, *4*, 87–99.

Wißkirchen, K., M. Tum, K. P. Günther, M. Niklaus, C. Eisfelder, and W. Knorr (2013), Quantifying the carbon uptake by vegetation for Europe on a 1 km^2 resolution using a remote sensing driven vegetation model, *Geosci. Model Dev.*, *6*(5), 1623–1640.

Woodward, F. I., and B. G. Williams (1987), Climate and plant distribution at global and local scales, *Vegetatio*, *69*, 189–197.

Zhao, M., and S. W. Running (2010), Drought-induced reduction in global terrestrial net primary production from 2000 through 2009, *Science*, *329*, 940–943.

Zhao, M., F. A. Heinsch, R. R. Nemani, and S. W. Running (2005), Improvements of the MODIS terrestrial gross and net primary production global data set, *Remote Sens. Environ.*, *95*(2), 164–176.